Complex Dynamic Model of a Multi-phase Asynchronous Motor with Harmonic Injection

Roberto Zanasi, Giovanni Azzone

***Abstract*— In this paper a new complex dynamic model for multi-phase asynchronous motors has been presented using the Power-Oriented Graphs (POG) technique. This new model is obtained using a complex rectangular transformation that reduces the number of the used complex state space variables. The odd harmonic injection has also been considered in order to describe the most general dynamics of the machine by using a compact model. Finally some simulation results have been reported to prove the effectiveness of the new transformation and to show the contribution of the harmonic injection in terms of torque enhancement.**

I. INTRODUCTION

The benefits and the advantages of the multi-phase asynchronous machines are well know in literature, see [3] and [4], especially concerning the torque enhancement: this aspect makes these machines particularly suitable for high-power applications. Another additional degree of freedom of the concentrated-winding multi-phase machines that contributes to provide a higher density torque, is the odd order harmonic injection, widely described in literature in [5], [6], [7], [8] and [9] in the cases of limited number of stator and rotor phases.

The main focus of this paper is to obtain a new complex reduced dynamic model of a multi-phase asynchronous motor, considering an arbitrary number of stator and rotor phases together with the odd order harmonic injection. The dynamic equations of the system have been obtained using a "complex" state space transformation that reduces the number of the internal variables and the obtained model has been graphically represented using the Power-Oriented Graphs modeling technique: the result is a very compact and general model of the machine, that includes the multi-phase features, the complex transformation and the harmonic injection and that can be easily used to perform any simulations of the induction motors. The paper is organized as follows: in Section II the basic properties of the POG technique in the complex case are briefly presented. Section III introduces and describes the complex reduced dynamic equations of the considered system, putting in evidence the harmonic injection and its contribution in terms of torque enhancement. Last Section IV shows some simulation results.

II. POWER-ORIENTED GRAPHS

The Power-Oriented Graphs, see [1] and [2], is a graphical modeling technique suitable for modeling physical systems.

R. Zanasi and G. Azzone are with Faculty of Engineering, DII - Information Engineering Department, University of Modena e Reggio Emilia, Via Vignolese 905, 41100 Modena, Italy {roberto.zanasi, giovanni.azzone}@unimore.it.

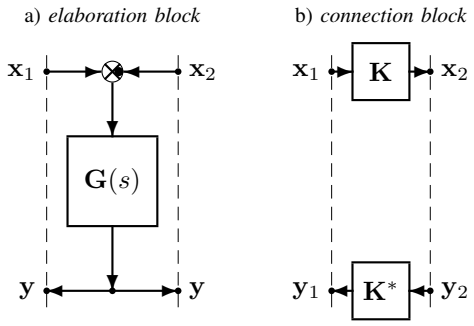

Fig. 1. POG: a) *elaboration block*; b) *connection block*.

The POG are normal block diagrams combined with a particular modular structure essentially based on the use of the two blocks shown in Fig. 1: the *elaboration block* stores and/or dissipates energy (i.e. springs, masses, dampers, capacities, inductances, resistances, etc.); the *connection block* redistributes the power within the system without storing or dissipating energy (i.e. any type of gear reduction, transformers, etc.). The POG schemes can be used both for scalar and vectorial systems, and for real and complex variables. In the vectorial case, $\mathbf{G}(s)$ and $\mathbf{K}$ are matrices: $\mathbf{G}(s)$ is always a square matrix of positive real transfer functions; matrix $\mathbf{K}$ can also be rectangular, time varying and function of other state variables. The circle present in the e.b. is a summation element and the black spot represents a minus sign that multiplies the entering variable. The main feature of the Power-Oriented Graphs is to keep a direct correspondence between the dashed sections of the graphs and real power sections of the modeled systems: the real part of the scalar product $\mathbf{x}^*\mathbf{y}$ of the two *power vectors* $\mathbf{x}$ and $\mathbf{y}$ involved in each dashed line of a power-oriented graph, see Fig. 1, has the physical meaning of *the power flowing through that particular section*. From the POG schemes one can directly obtain the state space equations of the system: $\mathbf{L}\dot{\mathbf{x}} = -\mathbf{A}\mathbf{x} + \mathbf{B}\mathbf{u}$, $\mathbf{y} = \mathbf{B}^*\mathbf{x}$. The *energy matrix* $\mathbf{L}$ is always symmetric and positive definite: $\mathbf{L} = \mathbf{L}^* > 0$. When an eigenvalue of matrix $\mathbf{L}$ tends to zero (or to infinity), the system degenerates towards a smaller dynamic system. The dynamic equations $\overline{\mathbf{L}}\dot{\mathbf{z}} = -\overline{\mathbf{A}}\mathbf{z} + \overline{\mathbf{B}}\mathbf{u}$ and $\mathbf{y} = \overline{\mathbf{B}}^*\mathbf{z}$ of the "reduced" system can always be obtained from the original one using a "congruent" transformation $\mathbf{x} = \mathbf{T}\mathbf{z}$ (matrix $\mathbf{T}$ can also be complex and/or rectangular) where $\overline{\mathbf{L}} = \mathbf{T}^*\mathbf{L}\mathbf{T}$, $\overline{\mathbf{A}} = \mathbf{T}^*\mathbf{A}\mathbf{T} - \mathbf{T}^*\mathbf{L}\dot{\mathbf{T}}$ and $\overline{\mathbf{B}} = \mathbf{T}^*\mathbf{B}$. When matrix $\mathbf{T}$ is rectangular, the system is transformed and reduced at the same time.

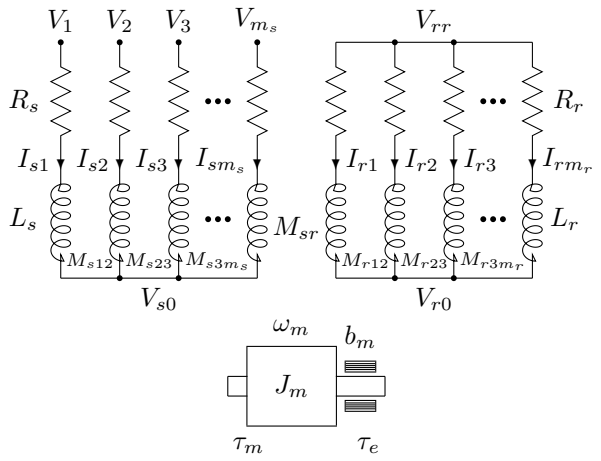

Fig. 2. Structure of a multi-phase asynchronous motor.

m_s	number of stator phases
m_r	number of rotor phases
p	number of rotor and stator polar expansions
γ_s	stator angular phase displacement ($\gamma_s = \frac{2\pi}{m_s}$)
γ_r	rotor angular phase displacement ($\gamma_r = \frac{2\pi}{m_r}$)
θ_m	rotor angular position
ω_m	rotor angular velocity
θ_s	stator voltage angular position
ω_s	stator voltage frequency
θ	electric angle ($\theta = p\,\theta_m$)
R_s	stator phases resistance
L_s	stator phases self inductance
M_{s0}	maximum mutual inductance of the stator phases
R_r	rotor phases resistance
L_r	rotor phases self inductance
M_{r0}	maximum mutual inductance of the rotor phases
M_{sr0}	stator-rotor phases maximum mutual inductance
J_m	rotor inertia momentum
b_m	rotor linear friction coefficient
τ_m	electromotive torque acting on the rotor
τ_e	external load torque acting on the rotor

TABLE I

ELECTRICAL AND MECHANICAL PARAMETERS OF THE MULTI-PHASE ASYNCHRONOUS MOTOR.

A. Notations

In this paper the following notations are used to denote full, diagonal, column and row matrices respectively:

$$\overset{i}{\underset{1:n}{[\![}}\, R_{i,j} \,\overset{j}{\underset{1:m}{]\!]}} = \begin{bmatrix} R_{11} & R_{12} \cdots & R_{1m} \\ R_{21} & R_{22} \cdots & R_{2m} \\ \vdots & \vdots \ddots & \vdots \\ R_{n1} & R_{n2} \cdots & R_{nm} \end{bmatrix}, \quad \overset{i}{\underset{1:n}{[\![}}\, R_i \,]\!] = \begin{bmatrix} R_1 & & \\ & \ddots & \\ & & R_n \end{bmatrix},$$

$$\overset{i}{\underset{1:n}{[\![}}\, R_i \,]\!] = \begin{bmatrix} R_1 & R_2 \cdots & R_n \end{bmatrix}^{\mathrm{T}}, \quad \underset{1:m}{[\![}\, R_j \,\overset{j}{]\!]} = \begin{bmatrix} R_1 & R_2 \cdots & R_m \end{bmatrix}.$$

The symbol $\delta(n)|_k^m$ denote the following function:

$$\delta(n)|_k^m = \begin{cases} 1 & \text{if } n \in [k,\, k \pm m,\, k \pm 2m, \ldots] \\ 0 & \text{in the other cases} \end{cases}$$

where $n, k, m \in \mathbb{Z}$. The symbol $\mathbf{I}_m$ denotes an identity matrix of order m.

III. COMPLEX DYNAMIC MODEL OF THE MOTOR

The structure of a multi-phase star-connected asynchronous motor is shown in Fig. 2, whose electrical and mechanical parameters are shown in Table I. All the electrical parameters have been obtained connecting in series the p polar couples of the motor. Let us denote ${}^t\mathbf{V}_s$, ${}^t\mathbf{I}_s$, ${}^t\mathbf{V}_r$ and ${}^t\mathbf{I}_r$ as stator and rotor voltage/current vectors in the external frame Σ_t:

$${}^t\mathbf{V}_s = \begin{bmatrix} V_{s1} \\ V_{s2} \\ \vdots \\ V_{sm_s} \end{bmatrix}, \; {}^t\mathbf{I}_s = \begin{bmatrix} I_{s1} \\ I_{s2} \\ \vdots \\ I_{sm_s} \end{bmatrix}, \; {}^t\mathbf{V}_r = \begin{bmatrix} V_{r1} \\ V_{r2} \\ \vdots \\ V_{rm_r} \end{bmatrix}, \; {}^t\mathbf{I}_r = \begin{bmatrix} I_{r1} \\ I_{r2} \\ \vdots \\ I_{rm_r} \end{bmatrix}$$

where $V_{si} = V_i - V_{s0}$ for $i \in \{1, 2, \ldots, m_s\}$ and $V_{ri} = V_{rr} - V_{r0}$ for $i \in \{1, 2, \ldots, m_r\}$. Using the following generalized state vector ${}^t\dot{\mathbf{q}}$ and extended input vector ${}^t\mathbf{V}$:

$${}^t\dot{\mathbf{q}} = \left[\begin{array}{c} {}^t\mathbf{I}_s \\ \hline {}^t\mathbf{I}_r \\ \hline \omega_m \end{array}\right] = \left[\begin{array}{c} {}^t\mathbf{I}_e \\ \hline \omega_m \end{array}\right], \qquad {}^t\mathbf{V} = \left[\begin{array}{c} {}^t\mathbf{V}_s \\ \hline {}^t\mathbf{V}_r \\ \hline -\tau_e \end{array}\right] = \left[\begin{array}{c} {}^t\mathbf{V}_e \\ \hline -\tau_e \end{array}\right]$$

and applying the "Lagrangian" approach discussed in [10], one obtains the following dynamic equations of the multi-phase asynchronous motor referred to the external frame Σ_t:

$$\frac{d}{dt}\Bigg(\underbrace{\left[\begin{array}{c|c} {}^t\mathbf{L}_e & 0 \\ \hline 0 & J_m \end{array}\right]}_{{}^t\mathbf{L}({}^t\mathbf{q})} \underbrace{\left[\begin{array}{c} {}^t\mathbf{I}_e \\ \hline \omega_m \end{array}\right]}_{{}^t\dot{\mathbf{q}}}\Bigg) = -\underbrace{\left[\begin{array}{c|c} {}^t\mathbf{R}_e + {}^t\mathbf{F}_e & {}^t\mathbf{K}_e \\ \hline -{}^t\mathbf{K}_e^{\mathrm{T}} & b_m \end{array}\right]}_{{}^t\mathbf{R} + {}^t\mathbf{W}} \underbrace{\left[\begin{array}{c} {}^t\mathbf{I}_e \\ \hline \omega_m \end{array}\right]}_{{}^t\dot{\mathbf{q}}} + \underbrace{\left[\begin{array}{c} {}^t\mathbf{V}_e \\ \hline -\tau_e \end{array}\right]}_{{}^t\mathbf{V}} \tag{1}$$

where:

$${}^t\mathbf{L}({}^t\mathbf{q}) = \left[\begin{array}{cc|c} {}^t\mathbf{L}_s & {}^t\mathbf{M}_{sr}^{\mathrm{T}}(\theta_m) & 0 \\ {}^t\mathbf{M}_{sr}(\theta_m) & {}^t\mathbf{L}_r & 0 \\ \hline 0 & 0 & J_m \end{array}\right] = \left[\begin{array}{c|c} {}^t\mathbf{L}_e & 0 \\ \hline 0 & J_m \end{array}\right],$$

$${}^t\mathbf{R} = \left[\begin{array}{cc|c} {}^t\mathbf{R}_s & 0 & 0 \\ 0 & {}^t\mathbf{R}_r & 0 \\ \hline 0 & 0 & b_m \end{array}\right] = \left[\begin{array}{c|c} {}^t\mathbf{R}_e & 0 \\ \hline 0 & b_m \end{array}\right],$$

$${}^t\mathbf{W} = \left[\begin{array}{cc|c} 0 & -\frac{1}{2}\,{}^t\dot{\mathbf{M}}_{sr}^{\mathrm{T}} & \frac{1}{2}\frac{\partial\,{}^t\mathbf{M}_{sr}^{\mathrm{T}}}{\partial\theta_m}\,{}^t\mathbf{I}_r \\ -\frac{1}{2}\,{}^t\dot{\mathbf{M}}_{sr} & 0 & \frac{1}{2}\frac{\partial\,{}^t\mathbf{M}_{sr}}{\partial\theta_m}\,{}^t\mathbf{I}_s \\ \hline -\frac{1}{2}\,{}^t\mathbf{I}_r^{\mathrm{T}}\frac{\partial\,{}^t\mathbf{M}_{sr}}{\partial\theta_m} & -\frac{1}{2}\,{}^t\mathbf{I}_s^{\mathrm{T}}\frac{\partial\,{}^t\mathbf{M}_{sr}^{\mathrm{T}}}{\partial\theta_m} & 0 \end{array}\right].$$

In order to provide an harmonic injection, the stator and rotor self and mutual inductance matrices can be expressed with the following odd terms Fourier series:

$${}^t\mathbf{L}_s = L_{s0}\,\mathbf{I}_{m_s} + M_{s0}\left|\left|\left[\sum_{n=1:2}^{m_s-2} a_n^s\,\cos(n\,(i-j)\gamma_s)\right]\right|\right|_{1:m_s}^{i\;\;j},$$

$${}^t\mathbf{L}_r = L_{r0}\,\mathbf{I}_{m_r} + M_{r0}\left|\left|\left[\sum_{n=1:2}^{m_r-2} a_n^r\,\cos(n\,(i-j)\gamma_r)\right]\right|\right|_{1:m_r}^{i\;\;j},$$

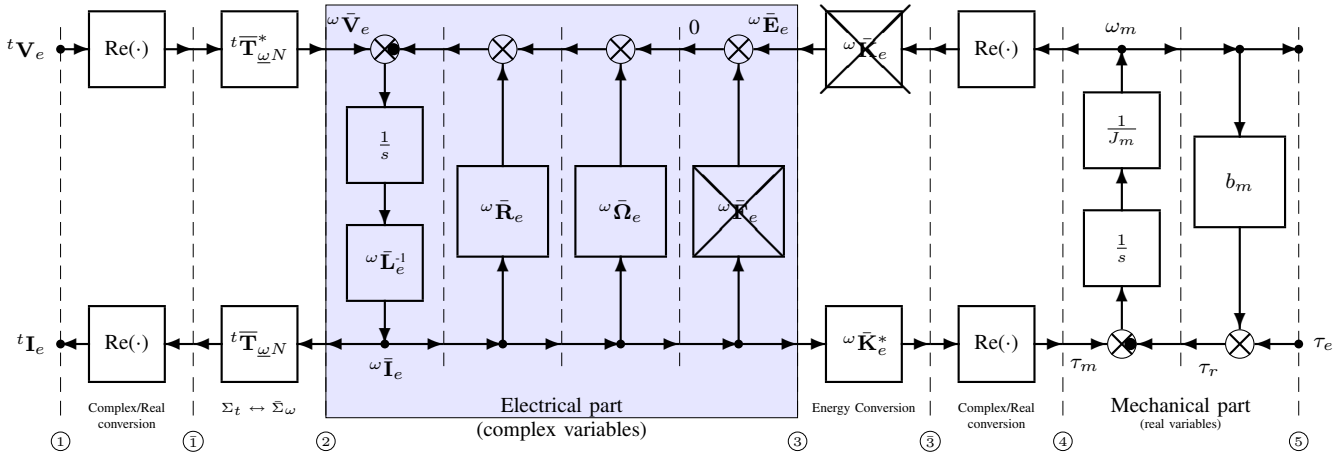

Fig. 3. POG graphical representation of a multi-phase asynchronous motor in the complex transformed frame $\bar{\Sigma}_\omega$.

$$ {}^{t}\mathbf{M}_{sr}(\theta) = M_{sr0} \left\| \left[\sum_{n=1:2}^{m_{sr}-2} a_n^{sr} \cos(n(\theta + i\gamma_r - j\gamma_s)) \right] \right\|_{0:m_s-1}^{j} \Bigg\|_{0:m_r-1}^{i} $$

where $m_{sr} = \min\{m_s, m_r\}$, $L_{s0} = L_s - M_{s0}$ and $L_{r0} = L_r - M_{r0}$. The terms a_n^s, a_n^r and a_n^{sr} are the coefficients of the self and mutual Fourier series. They satisfy the constraints:

$$ \sum_{n=1:2}^{m_s-2} |a_n^s| \leq 1, \qquad \sum_{n=1:2}^{m_r-2} |a_n^r| \leq 1, \qquad \sum_{n=1:2}^{m_{sr}-2} |a_n^{sr}| \leq 1. $$

The considered asynchronous motor belongs to the class of concentrated-winding multi-phase machines. Let ${}^{t}\tilde{\mathbf{T}}_\omega(m,\theta) \in \mathbb{C}^{m\times(m-1)/2}$ and ${}^{t}\tilde{\mathbf{T}}_{\underline{\omega}N} \in \mathbb{C}^{m\times(m+1)/2}$ denote the following rectangular "complex" matrices:

$$ {}^{t}\tilde{\mathbf{T}}_\omega(m,\theta) = \sqrt{\frac{1}{m}} \left\| \left[e^{j\,k(\theta - h\gamma_m)} \right] \right\|_{1:2:m-2}^{k} \Bigg\|_{0:m-1}^{h}, $$

$$ {}^{t}\tilde{\mathbf{T}}_{\underline{\omega}N}(m,\theta) = {}^{t}\tilde{\mathbf{T}}_{\underline{\omega}}(m,\theta)\,\mathbf{N}_m = \left[\begin{array}{cc} {}^{t}\tilde{\mathbf{T}}_\omega & \mathbf{z}_m \end{array} \right] \mathbf{N}_m \quad (2) $$

where $\gamma_m = \frac{2\pi}{m}$, $\mathbf{z}_m \in \mathbb{R}^m$ and $\mathbf{N}_m \in \mathbb{C}^{(m+1)/2\times(m+1)/2}$:

$$ \mathbf{z}_m = \left\| \left[\sqrt{\tfrac{1}{m}} \right] \right\|_{0:m-1}^{h}, \qquad \mathbf{N}_m = \left[\begin{array}{cc} \sqrt{2}\,\mathbf{I}_{\frac{m-1}{2}} & 0 \\ 0 & 1 \end{array} \right]. $$

Let ${}^{t}\mathbf{T}_\omega$ denote the following complex matrix, see (2):

$$ \begin{aligned} {}^{t}\mathbf{T}_\omega &= \left[\begin{array}{cc|c} {}^{t}\tilde{\mathbf{T}}_{\underline{\omega}N}(m_s,\theta_s) & 0 & 0 \\ 0 & {}^{t}\tilde{\mathbf{T}}_{\underline{\omega}N}(m_r,\theta_p) & 0 \\ \hline 0 & 0 & 1 \end{array} \right] = \left[\begin{array}{c|c} {}^{t}\overline{\mathbf{T}}_{\underline{\omega}N} & 0 \\ \hline 0 & 1 \end{array} \right] \\ &= \left[\begin{array}{cc|c} {}^{t}\tilde{\mathbf{T}}_{\underline{\omega}}(m_s,\theta_s) & 0 & 0 \\ 0 & {}^{t}\tilde{\mathbf{T}}_{\underline{\omega}}(m_r,\theta_p) & 0 \\ \hline 0 & 0 & 1 \end{array} \right] \left[\begin{array}{cc|c} \mathbf{N}_{m_s} & 0 & 0 \\ 0 & \mathbf{N}_{m_r} & 0 \\ \hline 0 & 0 & 1 \end{array} \right] \\ &= \left[\begin{array}{c|c} {}^{t}\overline{\mathbf{T}}_{\underline{\omega}} & 0 \\ \hline 0 & 1 \end{array} \right] \left[\begin{array}{c|c} \overline{\mathbf{N}} & 0 \\ \hline 0 & 1 \end{array} \right] = {}^{t}\overline{\mathbf{T}}_\omega\,\mathbf{N} \end{aligned} $$

where $\theta_p = \theta_s - \theta$. It can be easily shown that all the columns of matrix ${}^{t}\mathbf{T}_\omega$ are orthogonal complex vectors. Applying the state space transformation ${}^{t}\dot{\mathbf{q}} = {}^{t}\mathbf{T}_\omega^{*}\,{}^{\omega}\dot{\mathbf{q}}$ to system (1) one obtains the dynamic equations of the multi-phase asynchronous motor expressed in the new complex transformed frame $\bar{\Sigma}_\omega$:

$$ \underbrace{\left[\begin{array}{c|c} {}^{\omega}\bar{\mathbf{L}}_e & 0 \\ \hline 0 & J_m \end{array} \right]}_{{}^{\omega}\mathbf{L}} \underbrace{\left[\begin{array}{c} {}^{\omega}\dot{\bar{\mathbf{I}}}_e \\ \hline \dot{\omega}_m \end{array} \right]}_{{}^{\omega}\ddot{\mathbf{q}}} = - \underbrace{\left[\begin{array}{c|c} {}^{\omega}\bar{\mathbf{R}}_e + {}^{\omega}\bar{\mathbf{F}}_e + {}^{\omega}\bar{\mathbf{\Omega}}_e & {}^{\omega}\bar{\mathbf{K}}_e \\ \hline -{}^{\omega}\mathbf{K}_e^{*} & b_m \end{array} \right]}_{{}^{\omega}\mathbf{R} + {}^{\omega}\mathbf{W}} \underbrace{\left[\begin{array}{c} {}^{\omega}\bar{\mathbf{I}}_e \\ \hline \omega_m \end{array} \right]}_{{}^{\omega}\dot{\mathbf{q}}} + \underbrace{\left[\begin{array}{c} {}^{\omega}\bar{\mathbf{V}}_e \\ \hline -\tau_e \end{array} \right]}_{{}^{\omega}\mathbf{V}} \quad (3) $$

where: ${}^{\omega}\mathbf{L} = {}^{t}\overline{\mathbf{T}}_\omega^{*}\,{}^{t}\mathbf{L}\,{}^{t}\overline{\mathbf{T}}_\omega$, ${}^{\omega}\mathbf{R} = {}^{t}\overline{\mathbf{T}}_\omega^{*}\,{}^{t}\mathbf{R}\,{}^{t}\overline{\mathbf{T}}_\omega$ and ${}^{\omega}\mathbf{W} = {}^{t}\overline{\mathbf{T}}_\omega^{*}\,{}^{t}\mathbf{W}\,{}^{t}\overline{\mathbf{T}}_\omega$. The complex vectors ${}^{\omega}\mathbf{V} = {}^{t}\mathbf{T}_\omega^{*}\,{}^{t}\mathbf{V}$ and ${}^{\omega}\dot{\mathbf{q}} = {}^{t}\mathbf{T}_\omega^{*}\,{}^{t}\dot{\mathbf{q}}$ have the following structure:

$$ {}^{\omega}\mathbf{V} = \left[\begin{array}{c} {}^{\omega}\bar{\mathbf{V}}_s \\ \hline {}^{\omega}\bar{\mathbf{V}}_r \\ \hline -\tau_e \end{array} \right] = \left[\begin{array}{c} {}^{\omega}\bar{\mathbf{V}}_e \\ -\tau_e \end{array} \right], \qquad {}^{\omega}\dot{\mathbf{q}} = \left[\begin{array}{c} {}^{\omega}\bar{\mathbf{I}}_s \\ \hline {}^{\omega}\bar{\mathbf{I}}_r \\ \hline \omega_m \end{array} \right] = \left[\begin{array}{c} {}^{\omega}\bar{\mathbf{I}}_e \\ \omega_m \end{array} \right] $$

where ${}^{\omega}\bar{\mathbf{V}}_r = 0$ because the rotor phases are short-circuited. Moreover, vectors ${}^{\omega}\bar{\mathbf{I}}_e$ and ${}^{\omega}\bar{\mathbf{V}}_e$ have the following structure:

$$ {}^{\omega}\bar{\mathbf{I}}_e = {}^{t}\overline{\mathbf{T}}_{\underline{\omega}N}^{*}\,{}^{t}\mathbf{I}_e = \left[\begin{array}{c} {}^{t}\tilde{\mathbf{T}}_{\underline{\omega}N}^{*}(m_s,\theta_s)\,{}^{t}\mathbf{I}_s \\ \hline {}^{t}\tilde{\mathbf{T}}_{\underline{\omega}N}^{*}(m_r,\theta_p)\,{}^{t}\mathbf{I}_r \end{array} \right] = \left[\begin{array}{c} {}^{\omega}\bar{\mathbf{I}}_s \\ \hline {}^{\omega}I_{sm_s} \\ \hline {}^{\omega}\bar{\mathbf{I}}_r \\ \hline {}^{\omega}I_{rm_r} \end{array} \right], $$

$$ {}^{\omega}\bar{\mathbf{V}}_e = {}^{t}\overline{\mathbf{T}}_{\underline{\omega}N}^{*}\,{}^{t}\mathbf{V}_e = \left[\begin{array}{c} {}^{t}\tilde{\mathbf{T}}_{\underline{\omega}N}^{*}(m_s,\theta_s)\,{}^{t}\mathbf{V}_s \\ \hline {}^{t}\tilde{\mathbf{T}}_{\underline{\omega}N}^{*}(m_r,\theta_p)\,{}^{t}\mathbf{V}_r \end{array} \right] = \left[\begin{array}{c} {}^{\omega}\bar{\mathbf{V}}_s \\ \hline {}^{\omega}V_{sm_s} \\ \hline 0 \end{array} \right] $$

where ${}^{\omega}I_{sm_s} = \sum_{h=1}^{m_s} I_{sh}$, ${}^{\omega}I_{rm_s} = \sum_{h=1}^{m_r} I_{rh}$ and ${}^{\omega}V_{sm_s} = \sum_{h=1}^{m_r} V_{sh}$. When the stator and rotor phases are star-connected it is ${}^{\omega}I_{sm_s} = {}^{\omega}I_{rm_s} = 0$. When the input stator voltages are balanced it is $V_{sm_s} = 0$. Vectors ${}^{\omega}\bar{\mathbf{I}}_s$, ${}^{\omega}\bar{\mathbf{I}}_r$ and ${}^{\omega}\bar{\mathbf{V}}_s$ can be expressed as follows:

$$ {}^{\omega}\bar{\mathbf{I}}_s = \left\| \left[I_{dsk} + j\,I_{qsk} \right] \right\|_{1:2:m_s-2}^{k}, \qquad {}^{\omega}\bar{\mathbf{I}}_r = \left\| \left[I_{drk} + j\,I_{qrk} \right] \right\|_{1:2:m_r-2}^{k}, $$

$$ {}^{\omega}\bar{\mathbf{V}}_s = \left\| \left[V_{dsk} + j\,V_{qsk} \right] \right\|_{1:2:m_s-2}^{k}. $$

$$\left[\begin{array}{cc|c} L_{s0}+\frac{m_s}{2}M_{s0}\mathbf{a}_s & M_{sre}\mathbf{a}_{sr}^{\mathrm{T}} & 0 \\ M_{sre}\mathbf{a}_{sr} & L_{r0}+\frac{m_r}{2}M_{r0}\mathbf{a}_r & 0 \\ \hline 0 & 0 & J_m \end{array}\right]\left[\begin{array}{c} {}^{\omega}\dot{\bar{\mathbf{I}}}_s \\ {}^{\omega}\dot{\bar{\mathbf{I}}}_r \\ \hline \dot{\bar{\omega}}_m \end{array}\right]=-\left[\begin{array}{cc|c} R_s+j\omega_s\mathbf{k}_{m_s}(L_{s0}+\frac{m_s}{2}M_{s0}\mathbf{a}_s) & j\omega_s M_{sre}\mathbf{k}_{m_s}\mathbf{a}_{sr}^{\mathrm{T}} & 0 \\ j\omega_p M_{sre}\mathbf{k}_{m_r}\mathbf{a}_{sr} & R_r+j\omega_p\mathbf{k}_{m_r}(L_{r0}+\frac{m_r}{2}M_{r0}\mathbf{a}_r) & 0 \\ \hline j\frac{p}{2}M_{sre}{}^{\omega}\bar{\mathbf{I}}_r^*\mathbf{k}_{m_r}\mathbf{a}_{sr} & -j\frac{p}{2}M_{sre}{}^{\omega}\bar{\mathbf{I}}_s^*\mathbf{k}_{m_s}\mathbf{a}_{sr}^{\mathrm{T}} & b_m \end{array}\right]\left[\begin{array}{c} {}^{\omega}\bar{\mathbf{I}}_s \\ {}^{\omega}\bar{\mathbf{I}}_r \\ \hline \omega_m \end{array}\right]+\left[\begin{array}{c} {}^{\omega}\bar{\mathbf{V}}_s \\ 0 \\ \hline -\tau_e \end{array}\right]$$

Fig. 4. Complex dynamic equations of a multi-phase asynchronous motor with odd harmonic injection in the transformed reduced rotating frame $\bar{\Sigma}_\omega$.

In the transformed rotating frame $\bar{\Sigma}_\omega$ the energy matrix ${}^{\omega}\mathbf{L}$ has the following constant structure:

$${}^{\omega}\mathbf{L}=\left[\begin{array}{cc|c} L_{s0}+\frac{m_s}{2}M_{s0}\ \mathbf{a}_s & M_{sre}\ \mathbf{a}_{sr}^{\mathrm{T}} & 0 \\ M_{sre}\ \mathbf{a}_{sr} & L_{r0}+\frac{m_r}{2}M_{r0}\ \mathbf{a}_r & 0 \\ \hline 0 & 0 & J_m \end{array}\right]$$

where $\mathbf{a}_s$, $\mathbf{a}_r$ and $\mathbf{a}_{sr}$ are real constant matrices (function of the Fourier series coefficients) defined as follows:

$$\mathbf{a}_s=\Big\|\underset{1:2:m_s-2}{\overset{k}{[\![}}\ a_k^s\ \Big]\Big\|,\quad \mathbf{a}_r=\Big\|\underset{1:2:m_r-2}{\overset{k}{[\![}}\ a_k^r\ \Big]\Big\|,\quad \mathbf{a}_{sr}=\Big\|\underset{1:2:m_r-2\quad 1:2:m_s-2}{\overset{k}{[\![}}\ a_k^{sr}\ \delta(k)|_l^{\infty}\ \Big]\Big\|_{\,l}.$$

Matrix ${}^{\omega}\mathbf{W}$ has the following skew-symmetric structure:

$${}^{\omega}\mathbf{W}=\left[\begin{array}{cc|c} j\omega_s\mathbf{k}_{m_s}(L_{s0}+\frac{m_s}{2}M_{s0}\mathbf{a}_s) & j(\omega_s-\frac{\omega}{2})M_{sre}\mathbf{k}_{m_s}\mathbf{a}_{sr}^{\mathrm{T}} & {}^{\omega}\bar{\mathbf{K}}_s \\ j(\omega_s-\frac{\omega}{2})M_{sre}\mathbf{k}_{m_r}\mathbf{a}_{sr} & j\omega_p\mathbf{k}_{m_r}(L_{r0}+\frac{m_r}{2}M_{r0}\mathbf{a}_r) & {}^{\omega}\bar{\mathbf{K}}_r \\ \hline -{}^{\omega}\mathbf{K}_s^* & -{}^{\omega}\mathbf{K}_r^* & 0 \end{array}\right]$$

where $\mathbf{k}_m=\underset{1:2:m-2}{\overset{k}{[\![}}\ k\ ]\!]$. In the transformed frame $\bar{\Sigma}_\omega$ the torque vector ${}^{\omega}\bar{\mathbf{K}}_e^*$ has the following form:

$$\begin{aligned}{}^{\omega}\bar{\mathbf{K}}_e^* &= \left[\begin{array}{cc} {}^{\omega}\bar{\mathbf{K}}_s^* & {}^{\omega}\bar{\mathbf{K}}_r^* \end{array}\right] \\ &= \left[\begin{array}{c|c} -j\,\frac{p}{2}\,M_{sre}\,{}^{\omega}\bar{\mathbf{I}}_r^*\,\mathbf{k}_{m_r}\,\mathbf{a}_{sr} & j\,\frac{p}{2}\,M_{sre}\,{}^{\omega}\bar{\mathbf{I}}_s^*\,\mathbf{k}_{m_s}\,\mathbf{a}_{sr}^{\mathrm{T}} \end{array}\right].\end{aligned}$$

The mechanical torque τ_m can be expressed as:

$$\begin{aligned}\tau_m &= \mathrm{Re}\,({}^{\omega}\bar{\mathbf{K}}_e^*\,{}^{\omega}\mathbf{I}_e)=\mathrm{Re}\left(\left[\begin{array}{cc} {}^{\omega}\bar{\mathbf{K}}_s^* & {}^{\omega}\bar{\mathbf{K}}_r^* \end{array}\right]\left[\begin{array}{c} {}^{\omega}\bar{\mathbf{I}}_s \\ {}^{\omega}\bar{\mathbf{I}}_r \end{array}\right]\right) \\ &= \frac{p}{2}\,M_{sre}\,\mathrm{Re}\left(\left[-j\,{}^{\omega}\bar{\mathbf{I}}_r^*\,\mathbf{k}_{m_r}\,\mathbf{a}_{sr}\,\middle|\,j\,{}^{\omega}\bar{\mathbf{I}}_s^*\,\mathbf{k}_{m_s}\,\mathbf{a}_{sr}^{\mathrm{T}}\right]\left[\begin{array}{c} {}^{\omega}\bar{\mathbf{I}}_s \\ \hline {}^{\omega}\bar{\mathbf{I}}_r \end{array}\right]\right) \\ &= p\,M_{sre}\sum_{n=1:2}^{m_{sr}-2} k\,a_k^{sr}\,(I_{drk}\,I_{qsk}-I_{dsk}\,I_{qrk}).\end{aligned}\tag{4}$$

When the inductance matrices have a simple cosinusoidal shape, see [11], the expression of the mechanical torque is:

$$\begin{aligned}\tau_{m_1} &= \mathrm{Re}\,(\,j\,p\,M_{sre}\,{}^{\omega}\bar{\mathbf{I}}_s^*\,{}^{\omega}\bar{\mathbf{I}}_r)=\mathrm{Re}\,(\,j\,p\,M_{sre}\,{}^{\omega}\bar{I}_s^*\,{}^{\omega}\bar{I}_r) \\ &= p\,M_{sre}\,(I_{dr1}\,I_{qs1}-I_{ds1}\,I_{qr1}).\end{aligned}\tag{5}$$

In (5) the mechanical torque τ_{m_1} is generated only by the fundamental harmonic component, whatever is the number of stator and rotor phases. On the contrary, in (4) the mechanical torque is produced by all the odd harmonic components $n\in[1:2:m_{sr}-2]$, providing a higher torque density. A POG graphical representation of system (3) is shown in Fig. 3: the connection blocks present between sections ① and ② represent the state space transformation $\Sigma_t\leftrightarrow\bar{\Sigma}_\omega$. The connection block defined by function "Re(·)" represents the "complex to real conversion" of the input vectors. The elaboration blocks between sections ② and ③ represent the *Electrical part* of the system. This part is composed only by complex matrices and complex variables (see the lightly shaded section of Fig. 3). The *Mechanical part* of the motor is described by the blocks present between sections ④ and ⑤. The c.b. between sections ③ and ④ represents the energy and power conversion (without accumulation nor dissipation) between the electrical and mechanical domains. The expanded form of system (3) is shown in Fig. 4 where:

$$M_{sre}=\frac{M_{sr0}\sqrt{m_s m_r}}{2},\qquad \omega_p=\omega_s-\omega.$$

It can be easily proved that in (3) the two terms ${}^{\omega}\overline{\mathbf{K}}_e\,\omega_m$ and ${}^{\omega}\bar{\mathbf{F}}_e\,{}^{\omega}\bar{\mathbf{I}}_e$ simplify each other. These two terms have been left in the POG scheme of Fig. 3 and have been eliminated in the system equations represented in Fig. 4.

Electrical parameters	
$m_s=7$	$m_r=7$
$L_s=0.12$ mH	$L_r=0.12$ mH
$R_s=3\,\Omega$	$R_r=3\,\Omega$
$M_{s0}=0.1$ mH	$M_{r0}=0.1$ mH
$p=1$	$M_{sr0}=0.09$ mH
$V_{max}=100$ V	$\omega_s=8\pi$ rad/s
Mechanical parameters	
$J_m=0.8$ Kg m^2	$b_m=0.5$ Nm s/rad
$\tau_e=2$ Nm	

TABLE II
ELECTRICAL AND MECHANICAL PARAMETERS USED IN SUMULATION.

IV. SIMULATION RESULTS

This section presents the simulation results obtained in Matlab/Simulink by implementing the model of the motor discussed in Sec. III and shown in Fig. 3. The electrical and mechanical parameters used in simulation are listed in Tab. II. The considered input voltage vector has the following balanced structure:

$${}^{t}\mathbf{V}_s=\underset{1:7}{\overset{h}{[\![}}\ V_{sh}\ ]\!]=\sum_{k=1:2}^{5}\ \underset{1:7}{\overset{h}{[\![}}\ V_{mk}\cos(k\,(\theta_s-(h-1)\gamma_s))\ ]\!]\tag{6}$$

where $k\in[1:2:5]$ indicates the harmonic order. The mutual inductance coefficients ${}^{t}\mathbf{M}_{sr}(1,1)$ between the first stator and the first rotor phase are shown in Fig. 5: the different shapes have been obtained by using the following $\mathbf{a}_{sr}$ coefficient matrices: 1) $\mathbf{a}_{sr}=diag\left[\begin{array}{ccc}1 & 0 & 0\end{array}\right]$ which

corresponds to the fundamental harmonic injection only (blue curve of Fig. 5); 2) $\mathbf{a}_{sr} = diag\left[\begin{array}{ccc} 0.8 & 0.2 & 0 \end{array}\right]$, i.e. the fundamental plus 3^{rd} harmonic injection (green curve); 3) $\mathbf{a}_{sr} = diag\left[\begin{array}{ccc} 0.6 & 0.2 & 0.2 \end{array}\right]$, i.e. the fundamental plus 3^{rd} and 5^{th} harmonic injection (red curve). Clearly, the choice of the coefficients of $\mathbf{a}_{sr}$ is important to decide which weight has to be assigned to each harmonic in order to obtain the desired torque density, see (4). The following method has been adopted to define the input voltage vector amplitudes V_{mk} of (6): only the fundamental amplitude V_{m1} has been chosen, while the others have been scaled by using the following percentage coefficients K_1^k:

$$K_1^k = \frac{V_{mk}}{V_{m1}} = \frac{V_{dsk}}{V_{ds1}}, \qquad k \in \{3, 5\},$$

that indicate the percentage of the k^{th} harmonic component amplitude with respect to the fundamental. In Fig. 6 stator voltage V_{s1}, stator current I_{s1} and rotor current I_{r1} in the range $t \in [0, 1]$ s are shown, with $K_1^3 = V_{ds3}/V_{ds1} = 50\%$ and $K_1^5 = V_{ds5}/V_{ds1} = 33\%$: each curve refers to a different coefficient matrix $\mathbf{a}_{sr}$ previously defined, that is to a different mutual inductance shape of Fig. 5. Note that the lighter curves in Fig. 6 have a sinusoidal shape because they correspond to $\mathbf{a}_{sr} = diag\left[\begin{array}{ccc} 1 & 0 & 0 \end{array}\right]$, where only the fundamental has been considered. In Fig. 7 angular velocity ω_m and mechanical torque τ_m in the range $t \in [0, 1.8]$ s are shown, corresponding to the three different mutual inductance coefficients ${}^t\mathbf{M}_{sr}(1,1)$ shown in Fig. 5: it can be noticed that the mechanical torque τ_m is function of the number of odd harmonics involved, especially in terms of transient dynamics.

Let us now consider the following self and mutual inductance coefficient matrices:

$$\mathbf{a}_s = \mathbf{a}_r = \mathbf{a}_{sr} = diag\left[\begin{array}{ccc} 0.6 & 0.2 & 0.2 \end{array}\right],$$

and let us vary the scaling coefficients as follows:

$$K_1^3 = \left[\begin{array}{ccccc} 0 & 15 & 30 & 45 & 60 \end{array}\right]\%, \qquad K_1^5 = K_1^3/2.$$

In Fig. 8 the time behavior of V_{s1}, I_{s1} and I_{r1} in the range $t \in [0, 1]$ s have been reported as function of the scaling coefficients K_1^3 and K_1^5. The time behavior of mechanical torque τ_m and angular velocity ω_m in the frame $t \in [0, 1.8]$ s, are reported in Fig. 9: one can notice how the torque density increases by choosing higher values of coefficients K_1^k. This is well shown in Fig. 10, where a three-dimensional evolution of the mechanical torque as function of the angular velocity and the scaling coefficients are shown, together with the torque level curves: one can notice that the peak torque and the steady-state torque are both proportional to the coefficients K_1^k. Finally, in Fig. 11, steady-state torque τ_{ss} and peak torque τ_p are reported: the increase of the amplitude of the injected harmonics provide a significantly higher peak torque compared with the smaller variation of the steady-state torque.

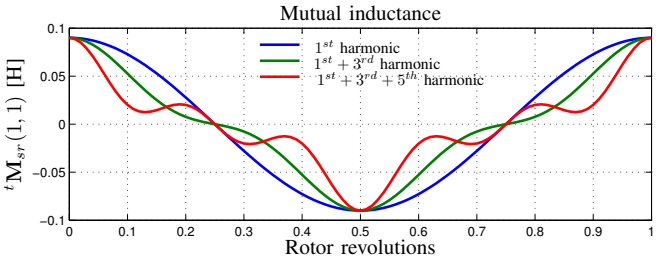

Fig. 5. Mutual inductance between the first stator and rotor phase.

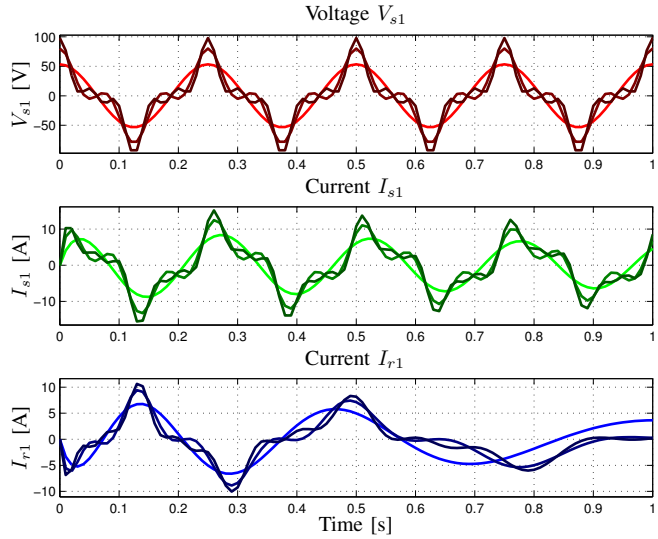

Fig. 6. Time behavior of stator voltage V_{s1}, stator current I_{s1} and rotor current I_{r1} in the original reference frame Σ_t as function of coefficient matrices $\mathbf{a}_{sr}$.

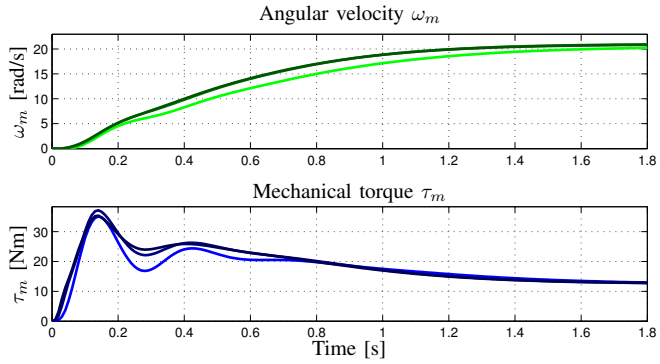

Fig. 7. Time behavior of angular velocity ω_m and mechanical torque τ_m as function of coefficient matrices $\mathbf{a}_{sr}$.

V. CONCLUSION

In the paper a compact and general complex dynamic model of a multi-phase asynchronous motor has been presented and modeled using the POG graphical technique. A complex rectangular transformation has been used and the odd harmonic injection terms have been considered, obtaining a reduced-order model that describes the dynamics of the asynchronous machine in the most general case. This model has been implemented in Matlab/Simulink and simulated in the 7-phase case. The simulation results have

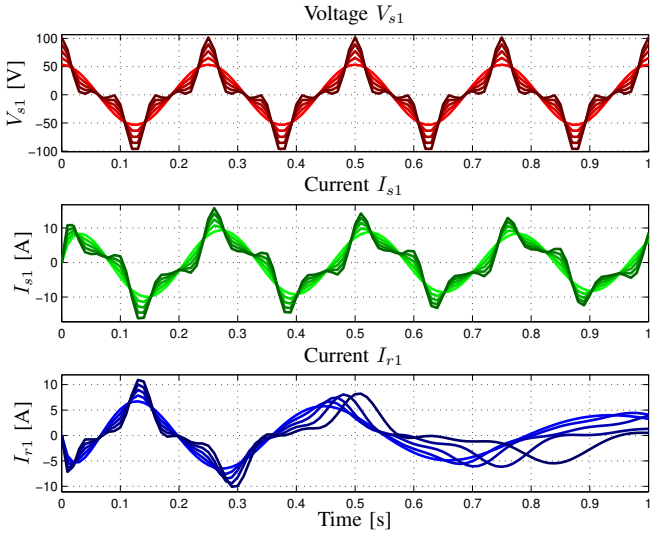

Fig. 8. Time behavior of stator voltage V_{s1}, stator current I_{s1} and rotor current I_{r1} in the original reference frame Σ_t as function of scaling coefficients K_1^3 and K_1^5.

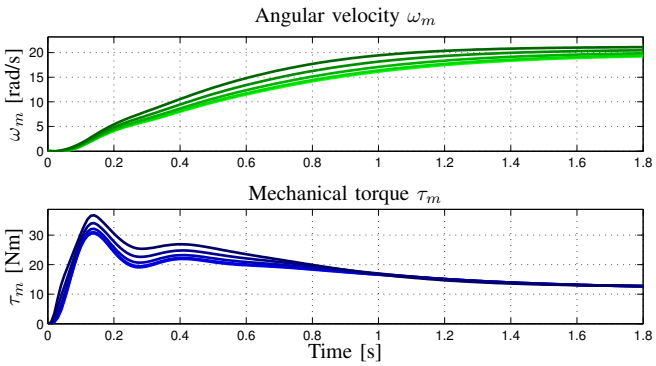

Fig. 9. Time behavior of angular velocity ω_m and mechanical torque τ_m as function of scaling coefficients K_1^3 and K_1^5.

shown the contribution of the harmonic injection in terms of torque enhancement and have depicted the different behaviors corresponding to the different harmonic order injected.

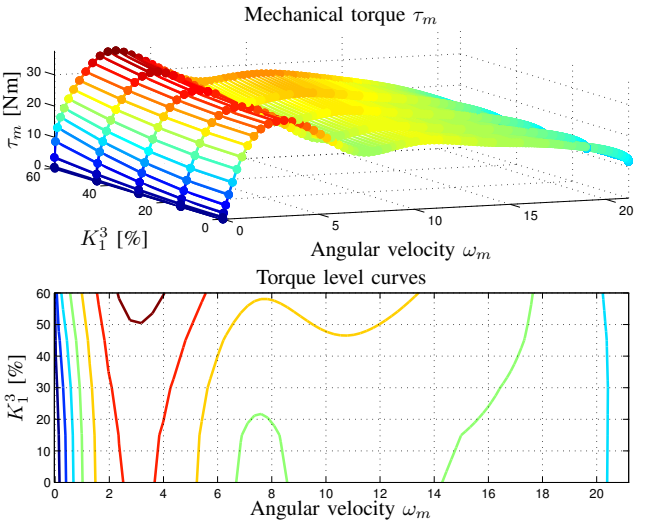

Fig. 10. Mechanical torque τ_m as function of angular velocity ω_m and scaling coefficients K_1^3 and K_1^5 ($K_1^5 = K_1^3/2$), and torque level curves.

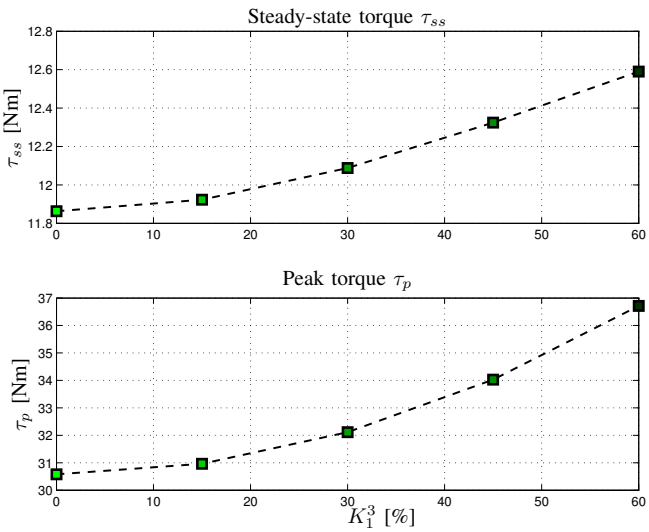

Fig. 11. Steady-state mechanical torque τ_{ss} and peak mechanical torque τ_p as function of scaling coefficients K_1^3 and K_1^5 ($K_1^5 = K_1^3/2$).

REFERENCES

[1] R. Zanasi, *Power Oriented Modelling of Dynamical System for Simulation*, *IMACS Symp. on Modelling and Control*, Lille, France, May 1991.

[2] R. Zanasi, *The Power-Oriented Graphs Technique: system modeling and basic properties*, *Vehicular Power and Propulsion Conference*, Lille, France, September 2010.

[3] G.K. Singh, *Multi-phase induction machine drive research - A survey*, *Electr. Power System Res.*, vol. 61, no. 2, pp. 139-147, March 2002.

[4] E. Levi, R. Bojoi, F. Profumo, H.A. Toliyat, S. Williamson, *Multiphase induction motor drives - A technology status review*, *IET Electr. Power Appl.*, vol. 1, no. 4, pp. 489-516, July 2007.

[5] H.A. Toliyat, T.A. Lipo, J.C. White, *Analysis of a Concentrated Winding Induction Machine for Adjustable Speed Drive Applications. Part I. Motor Analysis*, *IEEE Trans. Energy Conv.*, vol. 6, no. 4, pp. 679-683, December 1991.

[6] H.A. Toliyat, T.A. Lipo, J.C. White, *Analysis of a Concentrated Winding Induction Machine for Adjustable Speed Drive Applications. Part II. Motor Design and Performance*, *IEEE Trans. Energy Conv.*, vol. 6, no. 4, pp. 684-692, December 1991.

[7] M.J. Duran, F. Salas, M.R. Arahal, *Bifurcation Analysis of Five-Phase Induction Motor Drives With Third Harmonic Injection*, *IEEE Trans. Industr. Electr.*, vol. 55, no. 5, May 2008.

[8] H. Xu, H.A. Toliyat, L.J. Petersen, *Rotor Field Oriented Control of Five-phase Induction Motor with the Combined Fundamental and Third Harmonic Currents*, *Proc. IEEE APEC*, vol. 1, pp. 392-398, March 2001.

[9] L.A. Pereira, C.C. Scharlau, L.F.A. Pereira, J.F. Haffner, *Model of a Five-Phase Induction Machine Allowing for Harmonics in the Air Gap Field*, *IEEE Transactions on Energy Conversion*, vol. 21, no. 4, p. 891, December 2006.

[10] R. Zanasi, F. Grossi, G. Azzone, *The POG technique for Modeling Multi-phase Asynchronous Motors*, *5th IEEE International Conference on Mechatronics*, April 14-17, 2009, Málaga, Spain.

[11] R. Zanasi, G. Azzone, *Complex Dynamic Model of a Multi-phase Asynchronous Motor*, *ICEM - International Conference on Eletrical Machines*, September 6-8, 2010, Rome, Italy.

[12] R. Zanasi, G. Azzone, *Field Oriented Control of a Multi-phase Asynchronous Motor with Harmonic Injection*, *Submitted to* 18^{th} *IFAC World Congress*, 28 August - 2 September 2011, Milan, Italy.